ACS OMEGA

http://pubs.acs.org/journal/acsodf

Article

3-Methoxythiophene-Based Indophenine Reaction Generating an Isomeric Dynamic Equilibrium System

Yanying Wei and Hua Jiang*

Cite This: *ACS Omega* 2023, 8, 11021−11028

Read Online

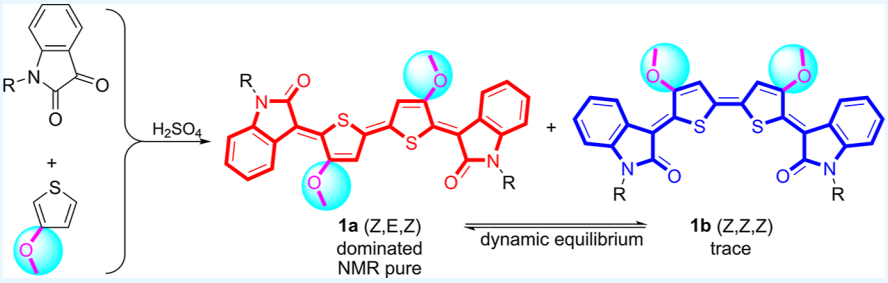

ABSTRACT: A 3-methoxythiophene-based indophenine reaction with *N*-(2-hexyldecyl)isatin in the presence of concentrated sulfuric acid produces an indophenine cis−trans isomeric dynamic equilibrium system, which is dominated by the (Z,E,Z) configuration with a trace of the (Z,Z,Z) configuration.

■ INTRODUCTION

The indophenine reaction, which is the reaction of isatin and thiophene promoted by concentrated sulfuric acid, has long been used to detect the presence of trace amounts of thiophene because the reaction results in a dramatic color change from red to blue.[1] Although the indophenine reaction was discovered as early as 1879,[2] the chemical structure of indophenine was not clarified until 1993.[3] As a class of indole derivative,[4−6] indophenine-based materials are being widely employed as organic semiconductors[7−12] or textile dyes[13−15] because of their unique characteristics and advantages, including simple synthesis, easy structural modification, a planar and rigid backbone, narrow energy-level band gap, and a high molar extinction coefficient.

However, further advances in the applications of indophenine are seriously hindered by the quinoidal cis−trans isomerism. Indophenine contains six isomers, and it is difficult to separate the isomers by conventional purification methods.[3] The formation of cis−trans isomers is related to the free rotation of the single bonds between each thiophene unit and isatin moiety during quinoidization. Introduction of appropriate steric substituents into the two thiophene units is known as an efficient strategy to eliminate isomerism. Li et al. reported an all-trans thiophene-*S*,*S*-dioxidized indophenine (**IDTO**) by oxidation post-modification and heating treatment on indophenine.[16] However, the intrinsic features of indophenine have been essentially changed in terms of the optophysical and electrochemical properties. Zhu et al. prepared an all-trans thieno[3,4-*b*]thiophene-based indophenine derivative (**DTIP**) via a complicated synthetic route instead of the indophenine reaction.[9] A much more ideal strategy to obtain indophenine derivatives without isomerism still is the indophenine reaction directly using thiophene derivatives containing steric substituents. In particular, all the indophenine reactions based on 3,4-propenedioxythiophene,[17] 3,4-ethylenedioxythiophene,[18] or even 3,4-dimethoxythiophene[19] have been recently demonstrated to produce indophenine derivatives with a specific (Z,E,Z) configuration along the quinoidal π-conjugation system (Figure 1).

Considering the role of alkoxy groups in controlling the indophenine backbone configuration, we are curious about how small a steric hindrance can effectively inhibit isomerization. For answering this question, we conducted a 3-methoxythiophene (3MeT)-based indophenine reaction to examine the effect of a single-alkoxy-group-substituted thiophene on isomerism. To our delight, the unsymmetric structure of 3MeT did not yield more indophenine isomers despite the six bonding modes available for the formation of the quinoidal bithiophene unit and the possible cis−trans isomerism between thiophene and isatin (Figure 2). In contrast, a (Z,E,Z) configuration-dominated indophenine (Z,E,Z)−(Z,Z,Z) isomeric dynamic equilibrium system was obtained as the reaction product (Scheme 1).

Received: December 6, 2022
Accepted: March 8, 2023
Published: March 16, 2023

https://doi.org/10.1021/acsomega.2c07767
ACS Omega 2023, 8, 11021−11028

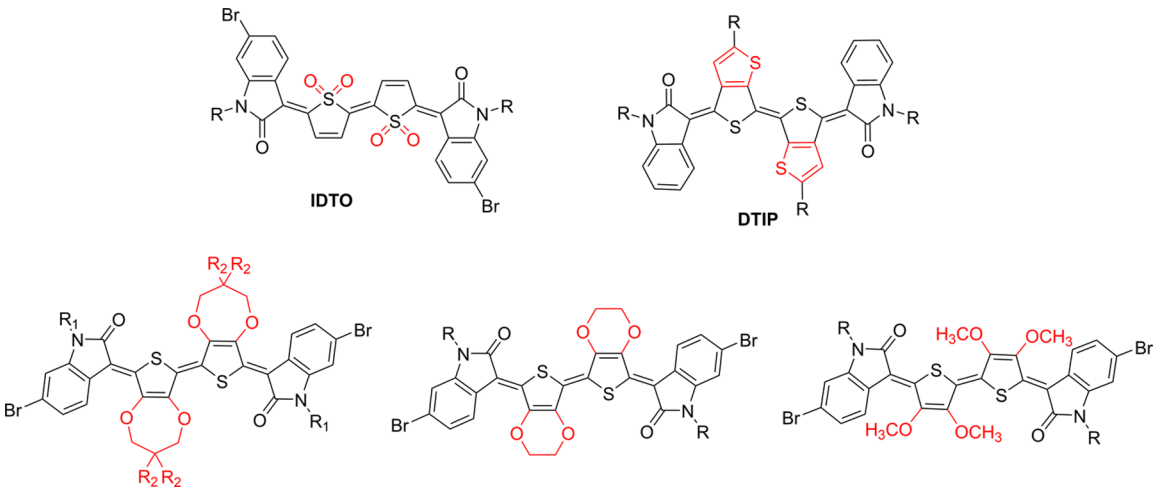

Figure 1. Structures of pure indophenine derivatives.

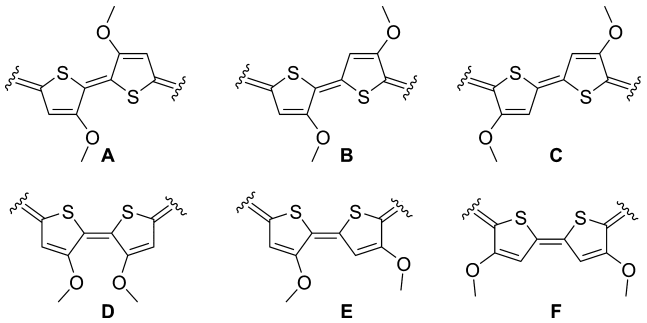

Figure 2. Bonding modes A−F for quinoidal bithiophene.

RESULTS AND DISCUSSION

Scheme 1 outlines the indophenine reaction based on 3MeT and *N*-(2-hexyldecyl)isatin in toluene in the presence of concentrated sulfuric acid. The 2-hexyldecyl group was used to increase the solubility of the final product, thus facilitating isolation. The thin layer chromatography (TLC) of the resultant mixture revealed a thick blue spot at the top position (**1a**) and a very light blue spot at the bottom position (**1b**). In particular, the main component **1a** was easily separated via column chromatography, although a trace amount of **1b** always accompanied. The ^{1}H nuclear magnetic resonance (NMR) spectrum of **1a** was well defined with only one singlet peak, two doublet peaks, and two triplet peaks in the aromatic region (Figure 3), clearly indicating the inhibition of isomers. The appearance of the singlet peaks at 6.83 ppm (H_m) and 4.07 ppm (H_n) was attributed to the protons on 3MeT, indicating a symmetric quinoidal bithiophene configuration. Compared with the H_a (7.60 ppm) of the isatin molecule, the H_f (8.16 ppm) of the indophenine molecule shifted downfield by 0.56 ppm owing to a partially negatively charged oxygen on the adjacent methoxy group.[20] This result implied that the two methoxy groups may be on the outside of the quinoidal bithiophene moiety[18] and that the structure may be in agreement with the (Z,E,Z) or (Z,Z,Z) configuration.

To further determine the position of the two methoxy groups, two-dimensional (2D) ^{1}H−^{1}H correlated spectroscopy (COSY) and nuclear Overhauser effect spectroscopy (NOESY) NMR spectra of **1a** were first recorded (Figure 4). The results showed no correlation between the protons on the thiophene and benzene rings. In addition, further oxidation of **1a** by *m*CPBA followed by heating produced one single product **2a** that was identified as an all-trans configuration, as previously reported.[16] An oxidized thiophene-based indophenine **2a′** without any methoxy group was also prepared for comparison.[21] It was observed that the H_o' peak (doublet, 8.69 ppm) for **2a′** disappeared in the NMR spectrum for **2a** and the

Scheme 1. Synthesis of 3MeT Indophenines 1a and 1b (Left) and the TLC (Right) Result for the Reaction Mixture

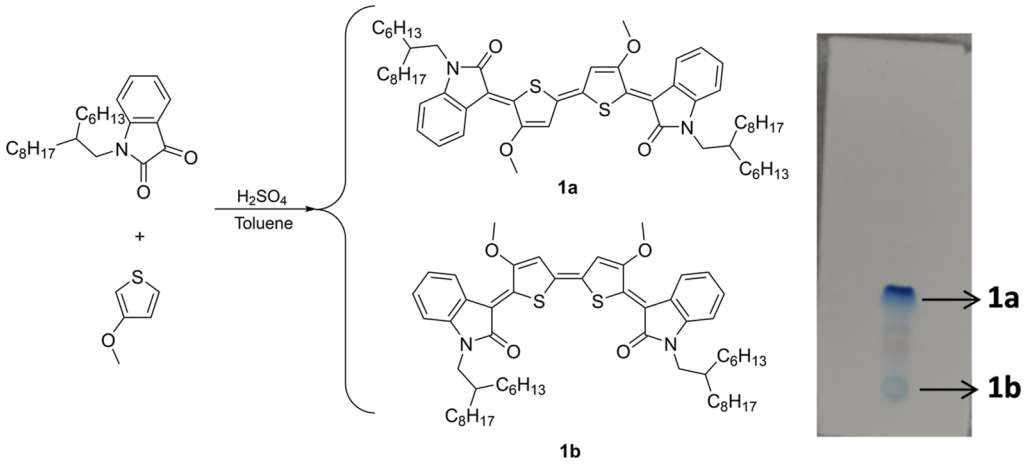

https://doi.org/10.1021/acsomega.2c07767
ACS Omega 2023, 8, 11021−11028

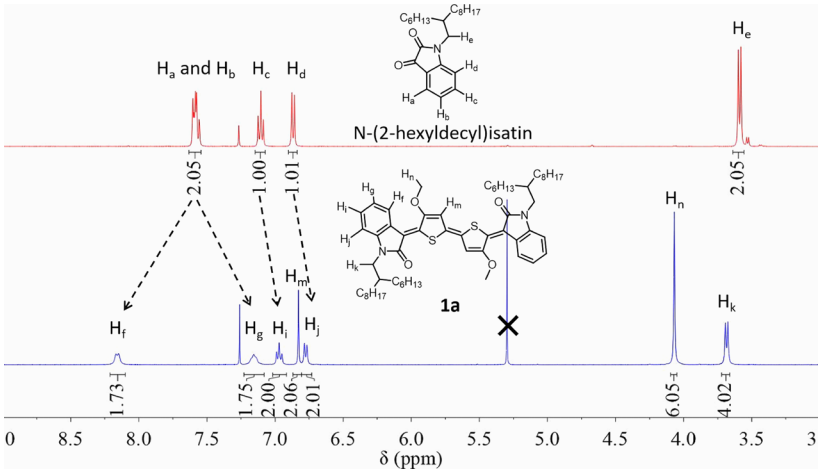

Figure 3. Partial ^{1}H NMR spectra for comparing the proton positions of *N*-(2-hexyldecyl)isatin and **1a** (9.0–3.0 ppm).

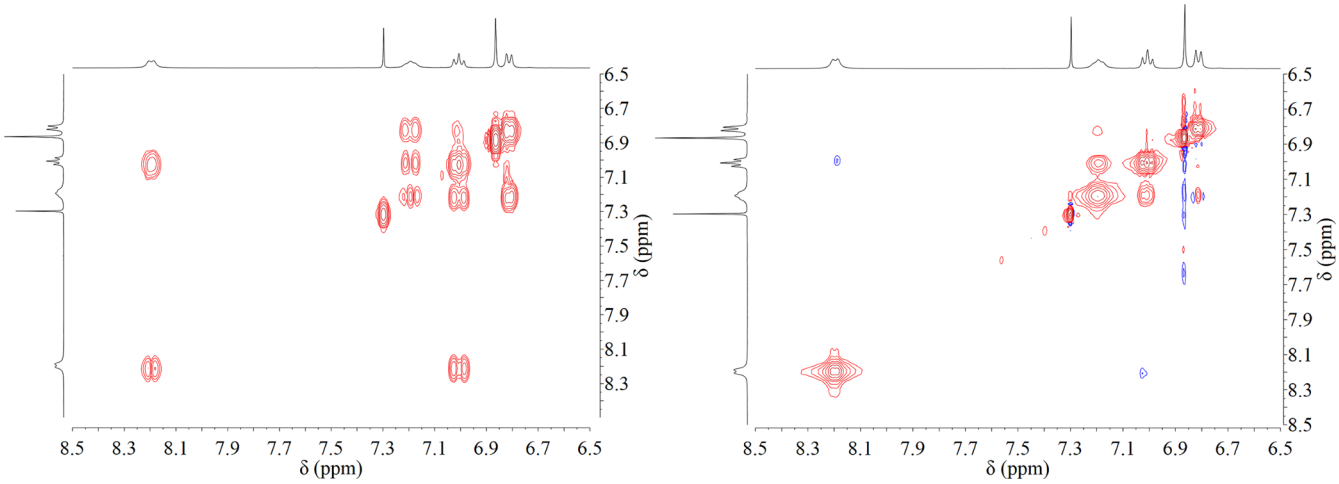

Figure 4. Partial 2D ^{1}H–^{1}H COSY (left) and NOESY (right) NMR spectra of **1a** (8.5–6.5 ppm).

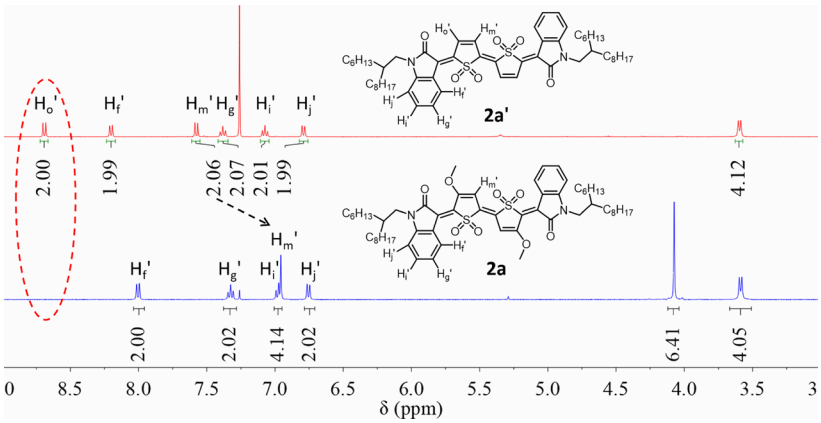

Figure 5. Partial ^{1}H NMR of indophenine derivatives **2a** and **2a′** (9.0–3.0 ppm).

H'_m peak (singlet, 6.96 ppm) in **2a** was located in the relatively high-field region—similar to the H'_m peak (doublet 7.58 ppm) for **2a′** (Figure 5). The chemical shift difference of the H_m' peak in **2a** and **2a′** was due to the shielding effect of the electron-donating methoxy group. Besides, the 2D ^{1}H–^{1}H COSY or NOESY NMR spectra of **2a** also did not show any correlation between the protons on thiophene and the benzene ring (Figure S3). Therefore, the two methoxy groups were speculated to lie on the two external positions of the quinoidal bithiophene.

The previously reported results indicated that the existence of alkoxy groups close to the isatin moiety forces the formation of a cis configuration between thiophene and isatin.[17−19] The same situation was observed in the case of 3MeT indophenine and was confirmed by monitoring the oxidation of **1a**. Although oxidation of **1a** to generate **2a** was observed to be

https://doi.org/10.1021/acsomega.2c07767
ACS Omega 2023, 8, 11021−11028

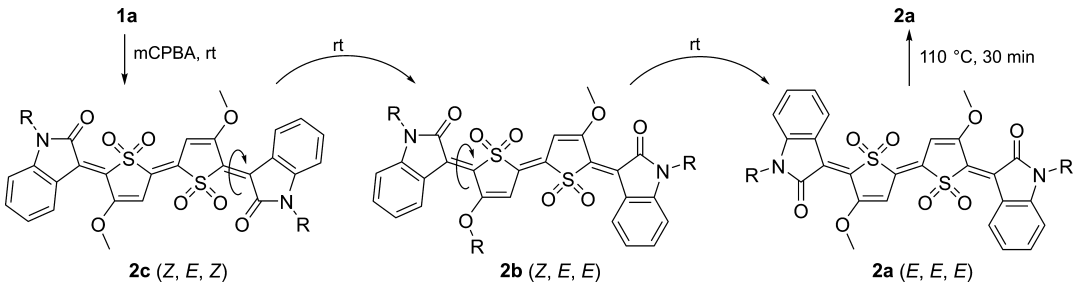

Figure 6. Oxidation of **1a** and the structural transformation of **2c** to **2a**.

relatively easy and fast because of the electron-donating property of the methoxy groups, the structural transformation was captured via the TLC (Figure S4). The primary oxidation product **2c** was gradually converted to a low-polarity substance **2b** and finally to **2a** over time.[16] After reaction for 60 min at room temperature (25 ± 5 °C), only **2a** existed; this situation did not change even after further heating at 110 °C for 30 min. Therefore, **2a**−**2c** were suggested to be (E,E,E), (Z,E,E), and (Z,E,Z) configurations, respectively. Thus, the structure of **2c** suggests the cis configuration between thiophene and isatin for **1a** (Figure 6).

Then, to verify the preference of 3MeT indophenine between the (Z,E,Z) and (Z,Z,Z) configurations, the energy information of the two configurations was calculated using the density functional theory (DFT) method[22] (Figure 7). The

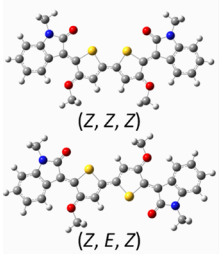

Total energy (Hartree)	Relative energy (kJ/mol)	Dipole moment (Debye)
−2286.52431	16.04	7.9925
−2286.53042	0	0.0005

Figure 7. Energy information of (Z,Z,Z) and (Z,E,Z) configurations.

(Z,E,Z) configuration had relatively lower energy than the (Z,Z,Z) configuration, with an energy difference of 16.04 kJ/mol. Moreover, the very low dipole moment of the (Z,E,Z) configuration was in accordance with the low polarity of **1a**. This result indicates that **1a** should exhibit the (Z,E,Z) configuration.

The small energy difference between (Z,E,Z) and (Z,Z,Z) suggests the existence of (Z,Z,Z). In fact, when the indophenine reaction product was examined by TLC, the spot with a higher polarity (**1b**) was found to be highly related to the (Z,Z,Z) configuration (Scheme 1). In one isolation operation, **1b** was carefully obtained with a yield of less than 1%. To our surprise, the most of the isolated **1b** had already converted to **1a**, resulting in a **1a**/**1b** mixture again, as confirmed by TLC (Figure S5). Besides, the isolated **1a** and **1b** also showed almost the same ^{1}H NMR spectra, high-resolution mass spectrometry (HRMS) result, elemental analysis result, infrared spectra, and UV−vis spectra (Figures S6−S9, Table S1). This meant that the cis configuration of the central double bonds was relatively unstable, and its conversion to the trans configuration was preferred (Figures S10 and S11). The balance ratio of **1b** to **1a** was calculated to be less than 1/55. Consequently, we could not characterize **1b** well. Although the newly isolated **1a** was also converted to a mixture of **1a** and **1b**, the trace amount of **1b** could not be easily distinguished from the NMR spectrum of **1a**.

The condition of 3MeT-based indophenine reaction was screened according to the yield of **1a** (Table S2). One equivalent of thiophene to isatin that dissolved in toluene, which reacted under the promotion of 10 equiv of sulfuric acid at 0 °C for 1 h, was regarded as the optimal condition for synthesizing **1a** with the best yield of 55%. In addition, the ratio of **1a** to **1b** did not show any obvious change throughout the condition-screening experiments.

Under the optimized reaction conditions, we explored the applicability of such 3MeT-based indophenine reaction for synthesizing indophenine derivatives (Scheme 2). Isatin derivatives containing methyl, methoxy, fluorine, or bromine were all capable of producing the corresponding 3MeT indophenine derivatives. Specifically, the ease of introduction of bromine atoms facilitated the rational design of 3MeT

Scheme 2. Synthetic Routes for Compounds 1 and 3−6

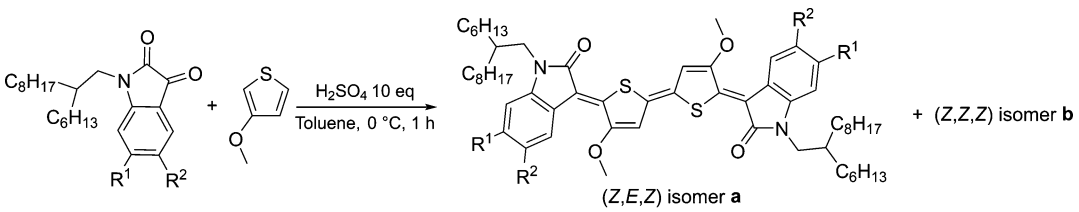

1 $R^1 = R^2 = H$; **1a** 55%, **1b** <1%; **1b**/**1a** < 1/55
3 $R^1 = H$, $R^2 = CH_3$; **3a** 53%, **3b** <1%; **3b**/**3a** < 1/53
4 $R^1 = H$, $R^2 = OCH_3$; **4a** 50%, **4b** <1%; **4b**/**4a** < 1/50
5 $R^1 = H$, $R^2 = F$; **5a** 47%, **5b** <1%; **5b**/**5a** < 1/47
6 $R^1 = Br$, $R^2 = H$; **6a** 48%, **6b** <1%; **6b**/**6a** < 1/48

https://doi.org/10.1021/acsomega.2c07767
ACS Omega 2023, 8, 11021−11028

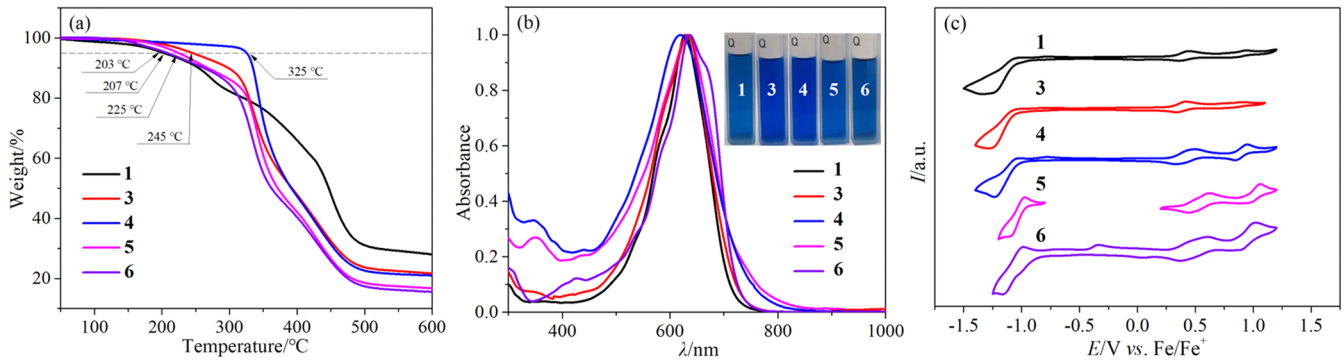

Figure 8. (a) TG curves, (b) ultraviolet (UV)−visible (vis) absorption spectra in DCM, and (c) CV curves for 3MeT indophenines.

Table 1. Optophysical and Electrochemical Data for 1 and 3−6

	λ_{max}/nm[a]	λ_{max}/nm[b]	ε/L·mol^{-1}·cm^{-1}	$\Delta\nu_{1/2}$/nm[a]	E_{HOMO}/eV[c]	E_{LUMO}/eV[c]	band gap/eV[d]
1	630	595 (850)	41 100	106	−4.97	−3.41	1.56
3	633	580	65 300	112	−4.97	−3.44	1.53
4	616	561	79 700	147	−4.91	−3.40	1.51
5	633	577	77 200	134	−5.12	−3.55	1.57
6	637	569	74 300	120	−5.09	−3.52	1.57

[a]Measured in CH_2Cl_2. [b]Recorded as film. [c]Calculated using the first oxidation/reduction potentials relative to ferrocene. [d]Band gap = $E_{LUMO} - E_{HOMO}$.

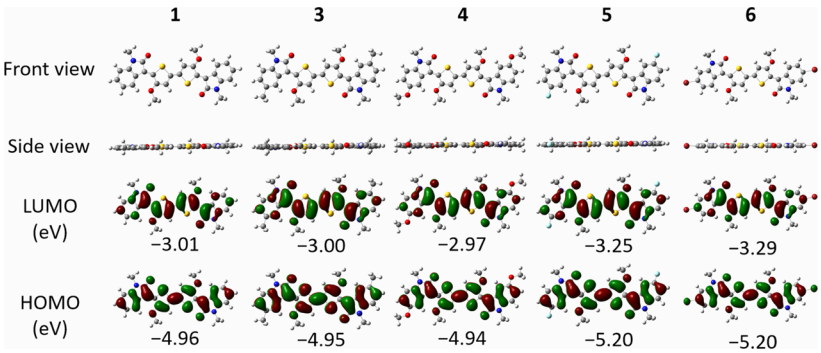

Figure 9. Low-lying ground-state molecular geometries and electron cloud density distributions for 3MeT indophenines.

indophenine-based materials.[18,19] Moreover, 5-methoxy isatin-based indophenine reaction had a relatively low reaction speed. Isatin was not completely consumed until 1.5 h, indicating the difficulty of protonation of 5-methoxy isatin because of the strong electron-donating property of the methoxy group. Similar to compound **1**, reaction products **3−6** also presented a (Z,E,Z)-configuration-dominated cis−trans isomerism equilibrium system, as indicated by their NMR spectra and calculation results (Table S3).

The thermogravimetric (TG) analyses of compounds **1** and **3−6** were recorded (Figure 8a). The results showed that the temperature of **1** at 5% weight loss was 203 °C. The introduction of the Br atom, F atom, methyl group, and methoxy group caused a gradual increase in the decomposition temperature to 207−325 °C. In particular, the introduction of methoxy groups in isatin moieties caused a drastic increase in the thermal decomposition temperature to 325 °C, which might be ascribed to the intramolecular interaction between methoxy groups (Figure S11). The high decomposition points of the 3MeT indophenines indicate their good thermal stability.

The optical properties were evaluated by recording the ultraviolet (UV)−visible absorption spectra (Figure 8b, Table 1). The blue 3MeT indophenine derivatives in dichloromethane exhibited an intense band because of the $\pi-\pi^*$ transition of the quinoidal thiophene system. Their maximum absorption wavelengths (λ_{max}) were in the range of 616−637 nm with molar extinction coefficients of 41 146−79 734 L·mol^{-1}·cm^{-1}. Among them, the methoxy-group-substituted 3MeT indophenine derivative showed the most blue-shifted λ_{max} of 616 nm, the highest ε of 79 734 L·mol^{-1}·cm^{-1}, and the widest $\Delta\nu_{1/2}$ of 147 nm. Compared with the absorption in the solution state, the absorption of the 3MeT indophenine as a film exhibited much broader curves (Figure S12). Their maximum absorption wavelengths blue-shifted with 33−64 nm, indicating their H-type aggregation in the solid state.[23]

The cyclic voltammetry (CV) curves of **1** and **3−6** in dichloromethane (10^{-3} mol·L^{-1}) showed that these compounds exhibited a one-electron oxidation process and a two-electron reduction process (Figure 8c). The highest occupied molecular orbital (HOMO) and lowest unoccupied molecular orbital (LUMO) energy levels for compound **1** were −4.97 and −3.41 eV, respectively, with a band gap of 1.56 eV (Table 1). The introduction of methyl and methoxy groups slightly increased the energy levels of the corresponding 3MeT indophenines because of their electron-donating property.

https://doi.org/10.1021/acsomega.2c07767
ACS Omega 2023, 8, 11021−11028

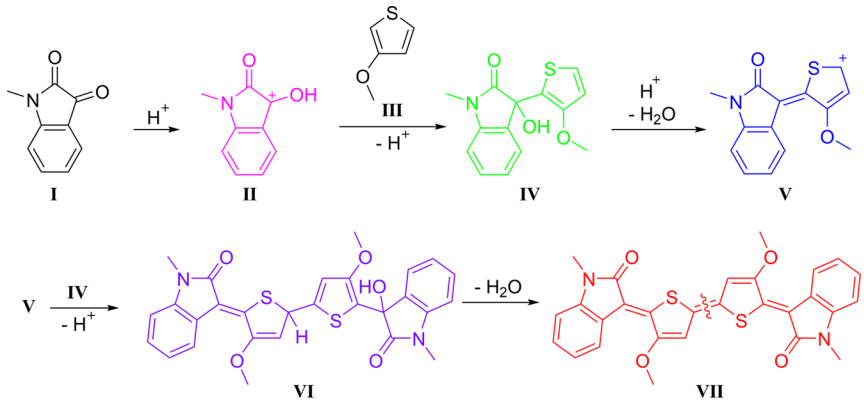

Figure 10. Proposed mechanism for the 3MeT-based indophenine reaction.

The HOMO energy levels for compounds **3** and **4** were −4.97 and −4.91 eV, respectively, while the LUMO energy levels were −3.44 and −3.40 eV, respectively. In contrast, when the F or Br atom was introduced, the HOMO energy levels for compounds **5** and **6** slightly decreased to −5.12 and −5.09 eV, respectively, while the LUMO energy levels slightly reduced to −3.55 and −3.52 eV, respectively. Nevertheless, their band gaps remained almost unchanged regardless of the effect of substituents.

To deeply understand the molecular geometries and electronic structures of the 3MeT indophenine derivatives, DFT calculations were performed at the B3LYP/6-311g++** level.[22] To simplify the calculations, the long alkyl chains were replaced by methyl groups (Figure 9). All atoms on the backbone of the 3MeT indophenine molecules were in the same plane as those containing the methoxy groups. It was thought that the high molecular planarity was beneficial to the intermolecular charge transfer. The HOMO and LUMO electron cloud densities were evenly distributed along the indophenine quinoidal π-conjugation system. The oxygen atoms on thiophene made a large contribution to both HOMO and LUMO. Therefore, the 3MeT indophenine derivatives exhibited relatively higher energy levels than the other reported indophenines.[16,17,21] The substituent effects on the HOMO/LUMO energy levels and band gap were consistent with the experimental results.

Based on the above experimental results and literature reports, we speculated that the mechanism of the 3MeT-based indophenine reaction was as follows (Figure 10). First, the 3-carbonyl group of isatin (**I**) was protonated to generate cation **II** under the promotion of a strong acid. Because of the high electron cloud density, the hydrogen at the 2-position in 3MeT was replaced by **II** to generate tertiary alcohol **IV**. Therefore, the two methoxy groups in the final indophenine structure were on the outside close to isatin. Alcohol **IV** reacted with the acid and dehydrated to form the cation **V**, which in turn attacked another **IV** to form **VI**. Finally, the dehydration of **VI** generated a long quinoidal π-conjugation system to yield blue indophenine compound **VII**, which mainly existed in the energetically stable (Z,E,Z) configuration because of the steric hindrance of methoxy groups.

■ CONCLUSIONS

In conclusion, 3MeT was demonstrated to effectively inhibit the isomerism of the indophenine reaction. The dominant (Z,E,Z) configuration of the 3MeT indophenines exhibited pure NMR spectra, although a trace of the (Z,Z,Z) configuration was always present. Interestingly, the (Z,Z,Z) isomer could not be well characterized because it tended to transform into the (Z,E,Z) isomer. Therefore, the production of an isomeric dynamic equilibrium system via the 3MeT-based indophenine reaction was demonstrated. The 3MeT indophenine derivatives exhibited high molecular planarity, low-energy electronic transitions, and amphoteric redox behavior, suggesting their promising application as organic optoelectronic materials.

■ EXPERIMENTAL SECTION

Materials and Methods. Isatin, thiophene, toluene, sulfuric acid (98% wt), and other chemicals were purchased from Adamas Reagent Co., Ltd. ^{1}H NMR, ^{13}C NMR spectra, 2D ^{1}H−^{1}H COSY, and NOESY NMR were recorded using an AVANCE AV400 MHz spectrometer. The absorption spectra were measured using a UV-756s UV spectrophotometer. The electro-chemical performance was investigated using a CHI1660 electrochemical workstation. The three-electrode CV system consists of glassy carbon (working electrode), platinum wire (auxiliary electrode), and saturated calomel (reference electrode). HRMS data were obtained by HRMS using a SYNAPT-G2-S HDMS spectrometer. Theoretical calculations were performed using Gaussian software.

General Procedure for the Synthesis of 3MeT Indophenine. Concentrated sulfuric acid (0.14 mL) was added to the toluene solution (1.25 mL) of the isatin derivative (0.25 mmol) and the 3-MeT (0.25 mmol) at 0 °C. The sulfuric acid phase immediately became blue-green and then blue. The mixture was stirred at 0 °C for 1 h until isatin was consumed as monitored by TLC. Then, ice water (100 mL) was added to quench the reaction. The reaction mixture was extracted with ethyl acetate (30 mL × 3), and the organic phase was combined and dried over anhydrous sodium sulfate. After removal of the organic solvent by evaporation under reduced pressure, the obtained crude product was further purified by silica gel chromatography (eluent for **1a**: $V_{\text{petroleum ether}}/V_{\text{ethyl acetate}}$ = 10/1; for **1b**: $V_{\text{petroleum ether}}/V_{\text{ethyl acetate}}$ = 10/3) to give the target blue 3MeT indophenines [a mixture of (Z,E,Z) and (Z,Z,Z) configurations].

1a, dark-blue solid, 64 mg, yield: 55%. mp: 95−97 °C. ^{1}H NMR ($CDCl_3$, 400 MHz): δ 8.16 (d, J = 7.2 Hz, 2H), 7.16 (dd, $J^1 = J^2$ = 6.8 Hz, 2H), 6.97 (dd, J^1 = 8.0 Hz, J^2 = 7.6 Hz, 2H), 6.83 (s, 2H), 6.78 (d, J = 7.6 Hz, 2H), 4.07 (s, 6H), 3.68 (d, J = 7.6 Hz, 4H), 1.91 (m, 2H), 1.30−1.22 (m, 48H), 0.87−

https://doi.org/10.1021/acsomega.2c07767
ACS Omega 2023, 8, 11021−11028

0.84 (m, 12H). ^{13}C NMR ($CDCl_3$, 100 MHz): δ 168.48, 162.60, 142.24, 142.05, 135.13, 127.61, 125.71, 122.02, 121.39, 113.95, 109.93, 108.25, 58.54, 44.86, 36.63, 31.97, 31.93, 31.86, 31.79, 30.03, 29.74, 29.57, 29.41, 29.33, 26.61, 22.71, 22.69, 14.16, 14.13. HRMS (ESI, m/z): calcd for $C_{58}H_{83}N_2O_4S_2$, 935.5794; found, 935.5756 [M + H]$^+$. **1b**, dark-blue solid, <1.0 mg, yield: <0.9%, this isolated substance quickly converted to the **1a**/**1b** equilibrium system.

3a, dark-blue solid, 65 mg, yield 53%. mp: 97−99 °C. ^{1}H NMR ($CDCl_3$, 400 MHz): δ 8.00 (s, 2H), 6.99 (d, J = 8.0 Hz, 2H), 6.84 (s, 2H), 6.69 (d, J = 8.0 Hz, 2H), 4.07 (s, 6H), 3.67 (d, J = 7.2 Hz, 4H), 2.36 (s, 6H), 1.91 (m, 2H), 1.29−1.22 (m, 48H), 0.87−0.84 (m, 12H). ^{13}C NMR ($CDCl_3$, 100 MHz): δ 168.50, 162.48, 141.91, 139.98, 135.01, 130.29, 128.09, 126.49, 122.03, 114.08, 109.82, 107.90, 58.35, 44.87, 36.60, 31.93, 31.86, 31.83, 31.77, 30.02, 29.74, 29.56, 29.33, 26.60, 22.70, 21.70, 14.15, 14.12, two aliphatic peaks are not shown due to the superimposition. HRMS (APCI, m/z): calcd for $C_{60}H_{87}N_2O_4S_2$, 963.6107; found, 963.6079 [M + H]$^+$. **3b**, dark-blue solid, <1.0 mg, yield: <0.8%, this isolated substance quickly converted to the **3a**/**3b** equilibrium system.

4a, dark-blue solid, 62 mg, yield 50%. mp: 100−102 °C ^{1}H NMR ($CDCl_3$, 400 MHz): δ 7.85 (s, 2H), 6.84 (s, 2H), 6.74 (d, J = 8.0 Hz, 2H), 6.66 (d, J = 8.0 Hz, 2H), 4.09 (s, 6H), 3.83 (s, 6H), 3.66 (d, J = 8.0 Hz, 4H), 1.90 (m, 2H), 1.29−1.22 (m, 48H), 0.84−0.85 (m, 12H). ^{13}C NMR ($CDCl_3$, 100 MHz): δ 168.26, 162.34, 154.54, 142.22, 136.30, 135.28, 122.56, 114.17, 113.13, 111.80, 109.90, 108.12, 58.62, 55.57, 44.86, 36.64, 32.01, 30.12, 29.82, 29.65, 29.42, 26.71, 22.78, 14.22. HRMS (APCI, m/z): calcd for $C_{60}H_{87}N_2O_6S_2$, 995.5963; found, 995.6000 [M + H]$^+$. **4b**, dark-blue solid, <1.0 mg, yield: <0.8%, this isolated substance would quickly convert to **4a**/**4b** equilibrium system.

5a, dark-blue solid, 57 mg, yield 47%. mp: 96−98 °C. ^{1}H NMR ($CDCl_3$, 400 MHz): δ 7.72 (dd, J^1 = 10.4 Hz, J^2 = 2.4 Hz, 2H), 6.77 (s, 2H), 6.74−6.71 (m, 2H), 6.55 (dd, J^1 = 8.4 Hz, J^2 = 4.8 Hz, 2H), 4.07 (s, 6H), 3.65 (d, J = 7.6 Hz, 4H), 1.85 (m, 2H), 1.28−1.22 (m, 48H), 0.87−0.84 (m, 12H). ^{13}C NMR ($CDCl_3$, 100 MHz): δ 168.22, 162.45, 157.00, 143.04, 138.06, 135.69, 122.49 (d, J = 9.9 Hz), 113.63, 113.38, 112.53, 110.07, 107.97 (d, J = 8.9 Hz), 58.61, 44.93, 36.56, 31.92, 31.84, 31.80, 30.02, 29.72, 29.55, 29.32, 26.60, 22.69, 22.67, 14.13, 14.11, two aliphatic peaks are not shown due to the superimposition. ^{19}F NMR ($CDCl_3$, 400 MHz): δ 122.37. HRMS (APCI, m/z): calcd for $C_{58}H_{81}F_2N_2O_4S_2$, 971.5606; found, 971.5561 [M + H]$^+$. **5b**, dark-blue solid, <1.0 mg, yield: <0.8%, this isolated substance quickly converted to the **5a**/**5b** equilibrium system.

6a, blue solid, 65 mg, yield 48%. mp: 97−99 °C. ^{1}H NMR ($CDCl_3$, 400 MHz): δ 7.82 (d, J = 8.0 Hz, 2H), 6.96 (d, J = 8.0 Hz, 2H), 6.72 (s, 2H), 6.69 (s, 2H), 4.05 (s, 6H), 3.56 (d, J = 7.2 Hz, 4H), 1.80 (m, 2H), 1.33−1.23 (m, 48H), 0.87−0.84 (m, 12H). ^{13}C NMR ($CDCl_3$, 100 MHz): δ 58.76, 44.87, 36.52, 32.04, 31.97, 31.86, 31.81, 30.13, 29.83, 29.69, 29.45, 26.64, 22.82, 14.26 (no peak was observed in the aromatic region). HRMS (APCI, m/z): calcd for $C_{58}H_{81}Br_2N_2O_4S_2$, 1093.3948; found, 1093.3979 [M + H]$^+$. **6b**, dark-blue solid, <1.0 mg, yield: <0.7%, this isolated substance quickly converted to the **6a**/**6b** equilibrium system.

■ ASSOCIATED CONTENT

Supporting Information

The Supporting Information is available free of charge at https://pubs.acs.org/doi/10.1021/acsomega.2c07767.

Details for the preparation of **2a**; 2D ^{1}H−^{1}H COSY and NOESY NMR spectra for **2a**; preparation of **2a′**; detection of the oxidation process from **1a** to **2a**; comparison of the TLC, ^{1}H NMR, HRMS, and elemental analysis results, IR spectra, and UV−vis spectra for **1a** and **1b**; reaction condition screening; effect of temperature and solvent on the ^{1}H NMR spectra of **1a**; energy and dipole moment information for the 3MeT indophenines; absorption spectra of the 3MeT indophenines as a film; NMR spectra of the 3MeT indophenine derivatives and isatin derivatives; and computational details and Cartesian coordinates for indophenine isomers (PDF)

■ AUTHOR INFORMATION

Corresponding Author

Hua Jiang − *Engineering Research Center for Eco-Dyeing and Finishing of Textiles, Ministry of Education, Zhejiang Sci-Tech University, Hangzhou 310018, China;* orcid.org/0000-0002-8530-9888; Email: jh@zstu.edu.cn

Author

Yanying Wei − *Engineering Research Center for Eco-Dyeing and Finishing of Textiles, Ministry of Education, Zhejiang Sci-Tech University, Hangzhou 310018, China*

Complete contact information is available at: https://pubs.acs.org/10.1021/acsomega.2c07767

Notes

The authors declare no competing financial interest.

■ ACKNOWLEDGMENTS

This work was supported by the National Natural Science Foundation of China (no. 21808210).

■ REFERENCES

(1) Moore, G. E. Report on the Progress of Analytical Chemistry. *J. Am. Chem. Soc.* **1879**, *1*, 320−380.

(2) Baeyer, A. Untersuchungen über die Gruppe des Indigblaus. *Ber. Dtsch. Chem. Ges.* **1879**, *12*, 1309−1319.

(3) Tormos, G. V.; Belmore, K. A.; Cava, M. P. The Indophenine Reaction Revisited. Properties of a Soluble Dialkyl Derivative. *J. Am. Chem. Soc.* **1993**, *115*, 11512−11515.

(4) Zhang, Y. C.; Jiang, F.; Shi, F. Organocatalytic Asymmetric Synthesis of Indole-Based Chiral Heterocycles: Strategies, Reactions, and Outreach. *Acc. Chem. Res.* **2020**, *53*, 425−446.

(5) Wang, Y.; Cobo, A. A.; Franz, A. K. Recent Advances in Organocatalytic Asymmetric Multicomponent Cascade Reactions for Enantioselective Synthesis of Spirooxindoles. *Org. Chem. Front.* **2021**, *8*, 4315−4348.

(6) Zhang, H. H.; Shi, F. Organocatalytic Atroposelective Synthesis of Indole Derivatives Bearing Axial Chirality: Strategies and Applications. *Acc. Chem. Res.* **2022**, *55*, 2562−2580.

(7) Hwang, H.; Khim, D.; Yun, J.-M.; Jung, E.; Jang, S.-Y.; Jang, Y. H.; Noh, Y.-Y.; Kim, D.-Y. Quinoidal Molecules as a New Class of Ambipolar Semiconductor Originating from Amphoteric Redox Behavior. *Adv. Funct. Mater.* **2015**, *25*, 1146−1156.

(8) Deng, Y.; Sun, B.; Quinn, J.; He, Y.; Ellard, J.; Guo, C.; Li, Y. Thiophene-S, S-dioxidized Indophenines as High Performance n-

Type Organic Semiconductors for Thin Film Transistors. *RSC Adv.* **2016**, *6*, 45410−45418.
(9) Ren, L.; Fan, H.; Huang, D.; Yuan, D.; Di, C.; Zhu, X. Dithienoindophenines: p-Type Semiconductors Designed by Quinoid Stabilization for Solar-Cell Applications. *Chem.—Eur. J.* **2016**, *22*, 17136−17140.
(10) Deng, Y.; Quinn, J.; Sun, B.; He, Y.; Ellard, J.; Li, Y. Thiophene-*S*, *S*-dioxidized indophenine (IDTO) based donor−acceptor polymers for n-channel organic thin film transistors. *RSC Adv.* **2016**, *6*, 34849−34854.
(11) Hwang, H.; Kim, Y.; Kang, M.; Lee, M.-H.; Heo, Y.-J.; Kim, D.-Y. A Conjugated Polymer with High Planarity and Extended π-Electron Delocalization via a Quinoid Structure Prepared by Short Synthetic Steps. *Polym. Chem.* **2017**, *8*, 361−365.
(12) Kim, Y.; Hwang, H.; Kim, N.-K.; Hwang, K.; Park, J.-J.; Shin, G.-I.; Kim, D.-Y. π-Conjugated Polymers Incorporating a Novel Planar Quinoid Building Block with Extended Delocalization and High Charge Carrier Mobility. *Adv. Mater.* **2018**, *30*, 1706557.
(13) Jiang, H.; Hu, Q.; Cai, J.; Cui, Z.; Zheng, J.; Chen, W. Synthesis and Dyeing Properties of Indophenine Dyes for Polyester Fabrics. *Dyes Pigm.* **2019**, *166*, 130−139.
(14) Cai, J.; Jiang, H.; Chen, W.; Cui, Z. Design, Synthesis, Characterization of Water-soluble Indophenine Dyes and Their Application for Dyeing of Wool, Silk and Nylon fabrics. *Dyes Pigm.* **2020**, *179*, 108385.
(15) Cai, J.; Jiang, H.; Cui, Z.; Chen, W. N-Sulphonatoalkyl Indophenine Derivatives: Design, Synthesis and Dyeing Properties on Wool, Silk and Nylon fabrics. *Color. Technol.* **2021**, *137*, 181−192.
(16) Deng, Y.; Sun, B.; He, Y.; Quinn, J.; Guo, C.; Li, Y. Thiophene-*S*, *S*-dioxidized Indophenine: A Quinoid-Type Building Block with High Electron Affinity for Constructing n-Type Polymer Semiconductors with Narrow Band Gaps. *Angew. Chem., Int. Ed.* **2016**, *55*, 3459−3462.
(17) Pappenfus, T. M.; Helmin, A. J.; Wilcox, W. D.; Severson, S. M.; Janzen, D. E. ProDOT-assisted Isomerically Pure Indophenines. *J. Org. Chem.* **2019**, *84*, 11253−11257.
(18) Hwang, K.; Lee, M.-H.; Kim, J.; Kim, Y.-J.; Kim, Y.; Hwang, H.; Kim, I.-B.; Kim, D.-Y. 3, 4-Ethylenedioxythiophene-based Isomer-free Quinoidal Building Block and Conjugated Polymers for Organic Field-effect Transistors. *Macromolecules* **2020**, *53*, 1977−1987.
(19) Sun, Y.; Zhang, Y.; Ran, Y.; Shi, L.; Zhang, Q.; Chen, J.; Li, Q.; Guo, Y.; Liu, Y. Methoxylation of Quinoidal Bithiophene as a Single Regioisomer Building Block for Narrow-bandgap Conjugated Polymers and High-performance Organic Field-effect Transistors. *J. Mater. Chem. C* **2020**, *8*, 15168−15174.
(20) Cao, Y.; Yuan, J.-S.; Zhou, X.; Wang, X.-Y.; Zhuang, F.-D.; Wang, J.-Y.; Pei, J. N-Fused BDOPV: a Tetralactam Derivative as a Building Block for Polymer Field-effect Transistors. *Chem. Commun.* **2015**, *51*, 10514−10516.
(21) Hu, Q.; Jiang, H.; Cui, Z.; Chen, W. An Insight Into the Effect of S, S-dioxided Thiophene on the Opto-physical/electro-chemical Properties and Light Stability for Indophenine Derivatives. *Dyes Pigm.* **2020**, *173*, 107891.
(22) Frisch, M. J.; Trucks, G. W.; Schlegel, H. B.; Scuseria, G. E.; Robb, M. A.; Cheeseman, J. R.; Scalmani, G.; Barone, V.; Mennucci, B.; Petersson, G. A.; Nakatsuji, H.; Caricato, M.; Li, X.; Hratchian, H. P.; Izmaylov, A. F.; Bloino, J.; Zheng, G.; Sonnenberg, J. L.; Hada, M.; Ehara, M.; Toyota, K.; Fukuda, R.; Hasegawa, J.; Ishida, M.; Nakajima, T.; Honda, Y.; Kitao, O.; Nakai, H.; Vreven, T.; Montgomery, J. A., Jr.; Peralta, J. E.; Ogliaro, F.; Bearpark, M.; Heyd, J. J.; Brothers, E.; Kudin, K. N.; Staroverov, V. N.; Kobayashi, R.; Normand, J.; Raghavachari, K.; Rendell, A.; Burant, J. C.; Iyengar, S. S.; Tomasi, J.; Cossi, M.; Rega, N.; Millam, J. M.; Klene, M.; Knox, J. E.; Cross, J. B.; Bakken, V.; Adamo, C.; Jaramillo, J.; Gomperts, R.; Stratmann, R. E.; Yazyev, O.; Austin, A. J.; Cammi, R.; Pomelli, C.; Ochterski, J. W.; Martin, R. L.; Morokuma, K.; Zakrzewski, V. G.; Voth, G. A.; Salvador, P.; Dannenberg, J. J.; Dapprich, S.; Daniels, A. D.; Farkas, O.; Foresman, J. B.; Ortiz, J. V.; Cioslowski, J.; Fox, D. J. *Gaussian 09*, Revision D.01; Gaussian, Inc.: Wallingford, CT, 2013.
(23) Cornil, J.; Beljonne, D.; Calbert, J.-P.; Brédas, J.-L. Interchain Interactions in Organic π-Conjugated Materials: Impact on Electronic Structure, Optical Response, and Charge Transport. *Adv. Mater.* **2001**, *13*, 1053−1067.

https://doi.org/10.1021/acsomega.2c07767
ACS Omega 2023, 8, 11021−11028